JOURNAL OF PROPULSION AND POWER
Vol. 25, No. 2, March–April 2009

Effects of Upstream Injection on Scramjet Performance Using an Entropy-Based Method

Matthew McGilvray* and Richard G. Morgan†
University of Queensland, St. Lucia, Queensland 4067, Australia

DOI: 10.2514/1.38325

Upstream injection has the potential for increasing the overall performance of a scramjet by reducing the overall length required to complete combustion and, thereby, reducing overall vehicle frictional drag. However, high flow losses will be incurred by injecting a fuel on the inlet where the Mach number is high. A simple overall approach based on entropy generation was used to investigate the effect of flow losses on overall performance. This showed that the injection flow losses can be quite high for upstream injection when compared with conventional combustor injection. An inviscid analysis of a two-dimensional scramjet at a Mach 10 flight condition found that a significant loss in overall performance of the engine occurs if the bulk of injection is undertaken on the intake. Estimates of viscous effects in a scramjet combustor showed that depending on the reduction of the mixing length achieved in the combustor, the upstream injection flow losses could be substantially recovered, making it an advantageous design option. The analysis technique developed, like similar simple analysis methodologies, provides a useful understanding of the physical processes that influence thrust production and can also be used to quickly evaluate and optimize potential configurations before starting detailed flowfield simulations.

Nomenclature

A	=	area, m^2
c_p	=	specific heat for constant pressure, $J/kg \cdot K$
F	=	thrust, N
H	=	stagnation enthalpy ($c_p T_s$), kJ/kg
I_{sp}	=	fuel specific impulse, s
L_{br}	=	length before reaction, m
L_i	=	ignition length, m
L_r	=	reaction length, m
$\dot{m}$	=	mass flow rate, kg/s
p	=	pressure, Pa
q	=	heat released, J
Q_f	=	energy added through combustion, kJ/kg
R	=	gas constant, $J/kg \cdot K$
T	=	temperature, K
U	=	velocity, m/s
x_c	=	axial distance from start of combustor, m
β	=	fuel injection angle to local flow, degrees
γ	=	specific heat ratio
Δs	=	entropy rise, $J/kg \cdot K$
η_b	=	combustion efficiency
η_c	=	heat release coefficient
η_{KE}	=	kinetic energy efficiency
λ	=	stoichiometric mass ratio of hydrogen to air, 0.0292
ρ	=	density, kg/m^3
ϕ	=	fuel equivalence ratio ($\frac{\dot{m}_f}{\phi \dot{m}_\infty}$)

Subscripts

a	=	air inflow condition
b	=	air/fuel exit condition
c	=	combustor
f	=	fuel
i	=	inlet
n	=	expansion nozzle
o	=	overall performance
s	=	stagnation conditions
1, 2, 3, 4	=	positions through scramjet
∞	=	freestream conditions

Received 9 June 2008; revision received 24 November 2008; accepted for publication 24 November 2008.

*Research Fellow, Centre for Hypersonics, Division of Mechanical Engineering. Member AIAA.

†Professor, Centre for Hypersonics, Division of Mechanical Engineering. Associate Fellow AIAA.

I. Introduction

SCRAMJET technology still requires substantial work on both subsystems and integration to become a viable option over conventional rockets. Upstream injection uses fuel injection on the intake of the scramjet, in contrast to the conventional use of injection inside the combustor. Upstream injection is a technique that has been explored for use in detonation-wave ramjets [1] to both inject and mix the fuel before the steady state detonation wave where the combustor would be in a scramjet. Upstream injection has been investigated as a possible way to increase the thrust potential in scramjet engines [2]. This is due to an increased distance to mix the fuel before reaching the high temperature and pressure conditions present in the combustor. Also, increased turbulent mixing should be possible due to the production of unsteady shock motions, especially through the strongest shock produced at the throat [3].

The flight regime that this technology may be applied to may be at higher flight velocities where significant reductions may be made in terms of frictional drag (long combustors and high velocity). The gains made by reducing frictional losses, however, may be mitigated by flow losses incurred by injecting the fuel into the airstream on the inlet where the Mach number is significantly higher than in the combustor [1]. Also, substantial boundary layer separation behind the injection location is undesirable due to many reasons, including unstart of the intake [4].

Experimental testing of scramjets using upstream injection has been undertaken since the late 1980s [5]. Recent tests of complete scramjet configurations have shown the effectiveness of upstream injection to both ignite the fuel and obtain extensive combustion with relatively short combustors [2,6]. Other work has proceeded to investigate the effects of premature ignition due to upstream injection [7]. So far, however, the negative effects of using upstream injection have yet been fully addressed. The main questions of how much should be injected where, at what flow conditions, and how it should vary with flight conditions remain unanswered. The work within this paper explores these issues and the effects on overall scramjet performance using a relatively simple one-dimensional analysis of a

scramjet. This method should give engineering trends for further analysis required for accurate estimates of the thrust performance with various fuelling strategies for a specific scramjet design.

II. Entropy Generation Method for Prediction of Overall Performance

Many methodologies for estimating both component efficiencies and overall performance have been developed for scramjet engines. An overview of some of the more well-known methods is given here. Waltrup et al. [8] presented an overall performance indiction based on specific impulse by combining individual component efficiencies into a unified cycle analysis. This methodology can be used to optimize the design of a scramjet engine. Similar cycle analysis has been presented by Ikawa [9] whereby thrust is maximized for a specific engine configuration. Kerrebrock [10] used a similar methodology to quantify the effects of finite rate chemistry on performance.

More recently Riggins et al. [11] introduced a methodology of evaluating thrust losses from the ideal scramjet engine in terms of irreversible entropy generation and incomplete combustion. This provides a basis for engine cycle analysis whereby thrust losses through the engine can be evaluated and summed together. This work was further extended by Riggins [12] to include the ability to evaluate performance for the multidimensional flows expected in scramjet engines.

Curran et al. [13] proposed a very simple method based on kinetic energy, which was reviewed by Heiser and Pratt [14]. This methodology assumes constant gas properties throughout the cycle and groups the individual component efficiencies into an overall parameter. This was based on the original thermodynamic cycle analysis of high-speed engines performed by Builder [15]. The overall performance [Eq. (1)] can be written in terms of the overall kinetic energy efficiency [Eq. (2)]. Looking at this equation shows that the overall performance can be written in terms of the amount of fuel injected and combustion properties, freestream conditions, and the performance efficiency term $\eta_{\mathrm{KE},o}$. Although simple, it has been shown that it can estimate the performance of scramjet configurations that have been tested experimentally. It was noted by Curran et al. [13], however, that this method can be disadvantageous with component efficiencies always close to 1.0, therefore, requiring a high degree for accurate inclusion

$$\frac{F}{\dot{m}_\infty} = U_\infty \left\{ \sqrt{\eta_{\mathrm{KE},o}(1+\lambda\phi)\left(1+\frac{\eta_b \lambda \phi Q_f}{c_p T_{s,\infty}}\right)} - 1 \right\} \tag{1}$$

$$\eta_{\mathrm{KE},o} = \eta_{\mathrm{KE},i}\eta_{\mathrm{KE},c}\eta_{\mathrm{KE},n} \tag{2}$$

The entropy-based method proposed here is similar to that of Curran et al. [13], although entropy is used as the performance prediction variable instead of kinetic energy efficiency. This is more advantageous as entropy is a direct thermodynamic property, and losses can be easily calculated for each component. Also the range for these varies up from zero, therefore bypassing the issues found with kinetic energy efficiency. This method allows for simple summation of any entropy-generating features of the flow throughout the scramjet cycle as shown by Riggins et al. [11], which allows for accountability of different loss factors to the overall scramjet performance.

The idealized cycle for a scramjet (Fig. 1) in terms of entropy and temperature can be seen in Fig. 2. Isentropic compression raises the temperature and pressure of the airstream to point 2′, combustion to point 3′, and isentropic expansion back to point 4. In the ideal cycle it can be seen that the only losses are due to Rayleigh effects during the heat addition process. Losses during the compression are expected due to both shock and viscous interactions, which, therefore, raises the entropy and temperature to point 2. The combustion process is also nonideal, with friction and heat transfer losses as well as incomplete combustion. Although lower losses are expected in the expansion nozzle, this process is also nonideal and is usually restricted due to the flow not being fully expanded to match ambient pressure. If the scramjet nozzle design expanded the gas to ambient pressure, the exit area will be larger than the intake, incurring a large increase in the external drag on the vehicle.

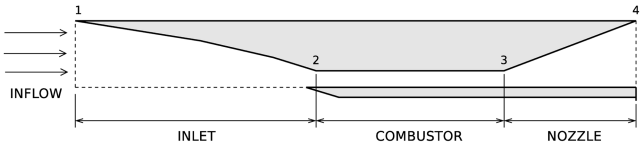

Fig. 1 Schematic of analytical representation of a scramjet.

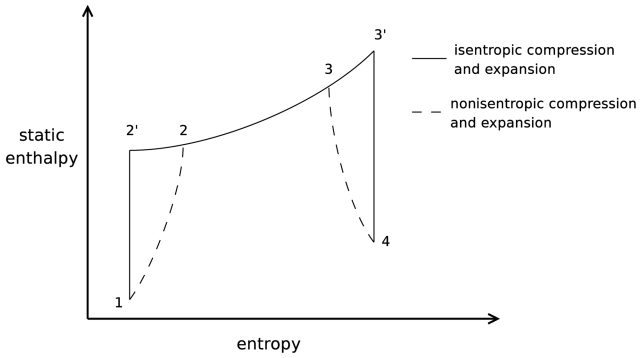

Fig. 2 Entropy–enthalpy cycle of a scramjet.

With the entropy-based method the thrust-per-unit intake area is given by Eq. (3), which is a function of the total entropy generation through the cycle [Eq. (4)]. This assumes constant gas properties throughout the cycle and expansion of the flow back to the same inlet capture area and ambient pressure. Thrust-per-unit intake area and specific impulse can be calculated for a specific flight condition and combustion properties in terms of the overall entropy generation. However, this must be adjusted, as currently both the area and pressure criteria at exit cannot be met. To calculate the properties at the exit plane, an adjustment must be made to how the flow is expanded as shown in Appendix A.

$$\frac{F}{\dot{m}_1} = \sqrt{(1+\lambda\phi)\frac{2\gamma R}{\gamma-1}\left[T_{s,1}\left(1+\frac{\eta_b\lambda\phi Q_f}{c_p T_{s,1}}\right) - (1+\lambda\phi)T_1 e^{\frac{\Delta s}{c_p}}\right]} - U_1 \tag{3}$$

$$\Delta s = \Delta s_{\mathrm{Rayleigh}} + \Delta s_{\mathrm{shock}} + \Delta s_{\mathrm{viscous}} + \Delta s_{\mathrm{injection}} + \ldots \tag{4}$$

A. Effect of Entropy on Thrust Generation for Example Conditions

A set of freestream conditions were calculated for a constant dynamic pressure flight path of 100 kPa shown in Table 1. As the vehicle ascends, the velocity increases while the pressure drops with the climbing altitude. Also shown is the predicted specific impulse predictions for a typical hydrogen-fuelled scramjet by Kors [16]. These are seen to decrease with the flight Mach number to quite low levels, although still higher than conventional chemical rockets.

Figure 3 shows the effect of entropy-raising processes on the performance (using the properties given in Table 2), without consideration of how they arise. It is evident that they are potentially

Table 1 Freestream properties for analysis and internal specific impulse prediction [16] for a H_2 fuelled scramjet

M_∞	h, km	U_∞, m/s	p_∞, Pa	T_∞, K	$H_{s,\infty}$, MJ/kg	$I_{\mathrm{sp,predicted}}$
8	27	2397	1903	223	3.097	2900
10	30	3016	1197	226	4.775	2250
12	32.5	3636	944	229	6.840	1750
15	34.5	4800	610	240	11.76	1250

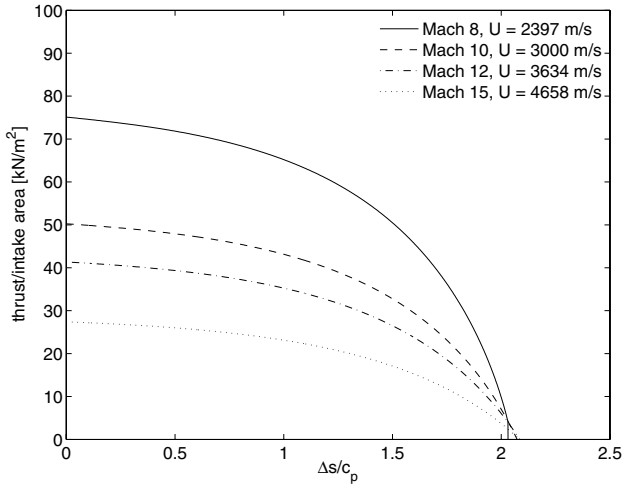

a) Thrust-per-unit intake area

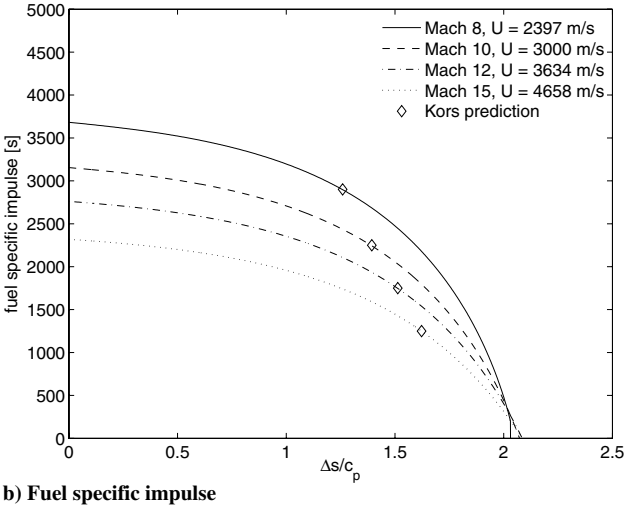

b) Fuel specific impulse

Fig. 3 Internal performance variation with entropy generated through scramjet cycle with thrust correction.

very significant and highly nonlinear in nature. The analysis also reveals that the overall entropy rise in a scramjet engine is limited to 2000 J/kg · K for all Mach numbers. As expected, the thrust potential is higher when the scramjet is at a lower speed. It also becomes apparent that if the entropy is already high due to unavoidable entropy generation, any slight increase will adversely affect performance. The purpose of this analysis is to identify the contribution from different mechanisms and to provide a procedure for evaluating and optimizing the performances of different configurations.

B. Effect of Entropy Generation from Nonisentropic Compression and Combustion

An estimate can be made of the amount of entropy generation expected from the inviscid compression process and constant-area combustion to gauge the performance without any losses due to viscous effects, combustion inefficiencies, losses in the thrust nozzle, and fuel injection and mixing. Figure 4 shows the expected Mach

Table 2 Properties for overall thrust calculation

γ	1.4
c_p, J/kg · K	1004.5
Q_f, MJ/kg	90
ϕ	1.0
η_b	1.0

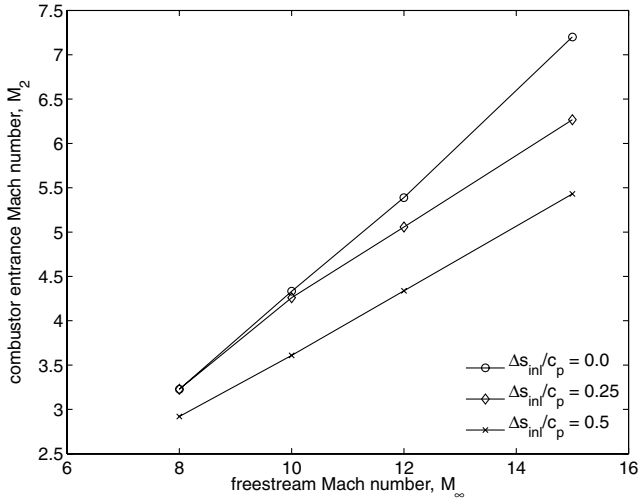

Fig. 4 Combustor-entrance Mach number with entropy generation from the inlet.

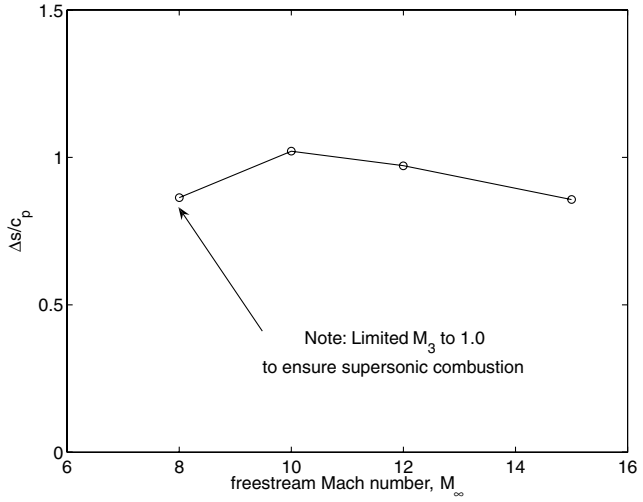

Fig. 5 Entropy generation by combustion using conditions with $\Delta s_{inl}/c_p = 0.25$.

number at the combustor entrance for various entropy generations on the inlet using the criteria that the pressure must be at least 100 kPa and temperature is at least 1000 K. These conditions are to ensure that the fuel reaches the autoignition conditions and reaches complete combustion without thermally chocking. The Mach number increases and is seen to be close to that approximated by Ferri [17].

An optimized, inviscid two-dimensional inlet with three external shocks and one internal shock has an approximate entropy rise of 270 J/kg · K for the prescribed compression. Therefore, using the conditions at the combustor inlet for $\Delta s/c_p$ of 0.25, the entropy generation can be calculated for constant-area heat addition in a frictionless duct, using the properties stated previously. This is shown in Fig. 5, where the Mach 8 condition case had to prevent subsonic flow. Thus, the entropy generation from the inlet shock compression and Rayleigh losses in combustion already have a significant impact on overall thrust with a $\Delta s/c_p$ of approximately 1.25. This means that entropy generation from these two sources can account for most of the entropy generation required to obtain the specific thrust predictions of Kors [16], especially at lower Mach numbers.

III. Entropy Generation for Constant-Pressure Mixing

To establish the contribution that fuel injection and mixing makes to total entropy generation, a quasi-one-dimensional discontinuity

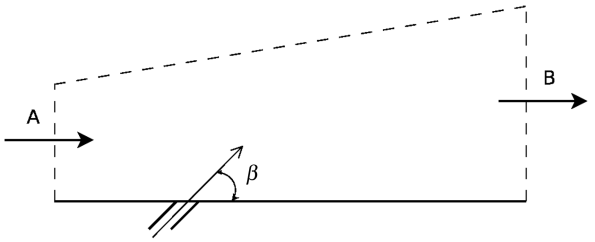

Fig. 6 Schematic of constant-pressure mixing analysis.

analysis is established as shown in Fig. 6. This analysis uses the conservation of mass, momentum, and energy, ignoring losses due to friction, nonuniform flow, and shocks.

The effect of the fuel-injection-interaction shock system is to initially compress and reduce the Mach number of the freestream gas. Although being a further source of entropy generation, lower entropy rises will be incurred from the fuel injection and mixing processes due to the reduction in the freestream Mach number. When targeting a given combustion chamber condition after injection, as some of the compression of the freestream will now be undertaken by the fuel injection shocks, there will be some degree of cancellation of the intake entropy rise due to a drop in the required intake compression. For the purposes of this analysis, all of the entropy increase is assumed to occur across the intake shock. If encouraging conditions are indicated, then it is worth doing a more complete and complex analysis. Attempting to add this level of complexity into this analytical model would loose the advantage of the simplicity and speed of use, while still not being a rigorous analysis.

This type of analysis was first explored for parallel injection on the inlet of a detonation-wave ramjet by Dunlap et al. [18]. Only negligible differences were seen between the constant-pressure and constant-area mixing, therefore the constant-pressure solution is investigated here due to the simplicity in formulation. With the physical injection, the incoming airflow, although achieving a higher pressure from passing through the injection interaction shock, will likely return to a slightly elevated pressure once expanded again, leading itself to the constant-pressure assumption. Separate studies have shown that the constant-pressure assumption does not greatly change the mixing-induced entropy rise, and so no correction is made for the freestream pressure rise by injection. The entropy generation across the injection and constant-pressure mixing is given by Eq. (5), with the formulation found in Appendix B. The fuel is assumed to be hydrogen, and so, therefore, change in the specific heat ratio is ignored

$$\frac{\Delta s}{c_{p,b}} = \ell_n \left\{ \frac{1}{T_a c_{p,b}} \left[\frac{H_a + \phi\lambda H_f}{1+\phi\lambda} - \left(\frac{U_a(1+\phi\lambda\frac{U_f}{U_a}\cos\beta)}{\sqrt{2}(1+\phi\lambda)} \right)^2 \right] \right\} \tag{5}$$

Using the nominal property values in Table 3 for the fuel at the point of injection and the initial freestream conditions in Table 1, a parametric study can be made of the influence of selected variables by perturbing each individually from the nominal value. The variables investigated were freestream condition, equivalence ratio, injection Mach number, fuel temperature, and injection angle. This analysis is shown in Fig. 7, where the entropy generation is given for a range of incoming air Mach numbers. With all variables the entropy generation from injection increases with incoming air Mach number. It is seen that there is a strong dependence on the freestream enthalpy, with lower enthalpy conditions (i.e., lower M_∞) generating larger entropies. For flight where the incoming Mach number (M_a) is conserved, the velocity of the flow at the mixing station will increase with the freestream Mach number ($M_i nfty$). The velocity of the fuel injection will stay the same, however, for the conditions stated here. Therefore, the proportional reduction in freestream momentum flux will be lower at the high values of the freestream Mach number, leading to reduced losses. The equivalence ratio also has a strong effect, with the entropy rising quite dramatically with the fuel equivalence ratio. Increasing the temperature of the fuel in this analysis will also increase the velocity and the resulting overall enthalpy. Therefore, any increase in temperature will increase the overall entropy generation. Entropy generation is not so strongly affected by the Mach number at which the fuel is injected or the angle.

Table 3 Nominal parameters of fuel at point of injection in constant-pressure mixing analysis

Freestream Mach number, M_∞	10
Freestream total enthalpy, H_∞	4.75 MJ/kg
Equivalence ratio, ϕ	1.0
Injection Mach number, M_f	1.0
Fuel temperature, T_f	1000 K
Injection angle, β	30 deg

The strong variation in entropy generation with fuel temperature is of importance for ground testing where the fuel has generally not been heated, causing higher performance characteristics. Even in the best case were the fuel is injected into the combustor ($M_a \sim 4.2$) the discrepancy between a fuel temperature of 300 K and likely flight temperatures of 1000 K gives a discrepancy in $\Delta s/c_p$ of 0.2. This is quite large and could lead to thrust inaccuracies of up to 20%. This is due to a larger exit temperature (T_b) with increasing fuel temperature, which creates a larger entropy generation as the process is at constant pressure. Riggins' [12] work predicts the opposite of this, although is not clear if the temperature discussed is the total or static temperature in the analysis.

The investigation of the interaction of these properties is difficult to comprehend from these basic performance plots. Therefore, the important properties of freestream condition and injection Mach number are visualized in three-dimensional plots for varying equivalence ratios and fuel temperatures (Fig. 8). It can be seen that the equivalence ratio gives a significant rise in entropy generation at lower values but then begins to plateau off. Also, the difference in entropy generation for variation in the fuel equivalence ratio is small at low inflow Mach numbers but becomes larger at higher inflow Mach numbers. Over the likely temperature range that scramjets may have for fuel injection in flight, the change in entropy generation is quite substantial. This, however, may be unavoidable due to thermal considerations in the design of an operational vehicle.

IV. Performance of Upstream Injection for Two-Dimensional Scramjet with Combustor Friction

The interplay between the injection and optimization of the inlet design is hard to predict from the presented results thus far. This is because the inlet design must be coupled to the compressive effects of upstream injection to achieve the required combustion chamber conditions. This decreases the losses due to fuel injection and mixing but increases the losses in the flow compression on the intake. Also, the mixing of the fuel and air stream is expected to increase the overall temperature before reaching the combustor, therefore requiring less compression of the flow on the intake if the fuel temperature is close to that expected in flight (approximately 1000 K).

A zero-dimensional inviscid analysis is undertaken on a generic scramjet configuration where the inlet consists of three external wedge compression surfaces and a single internal surface (Fig. 9). Conditions were set so that before combustion could take place, the static pressure has to be above 100 kPa and static temperature above 1000 K. The calculation first computes the conditions across the oblique shock using Rankine–Hugnoit equations [19], then the exit conditions from fuel injection and mixing with the equivalence ratio are defined for each surface. After this is completed for the four surfaces, combustion effects are calculated for a constant-area combustor by the addition of heat [19]. The combustion completion efficiency η_b was set to 0.6 to ensure that the flow does not become subsonic due to the overestimation of combustion effects. The freestream conditions were taken for the Mach 10 condition used previously. An optimization procedure was used were the external wedge angles were allowed to vary (internal angle is the summation

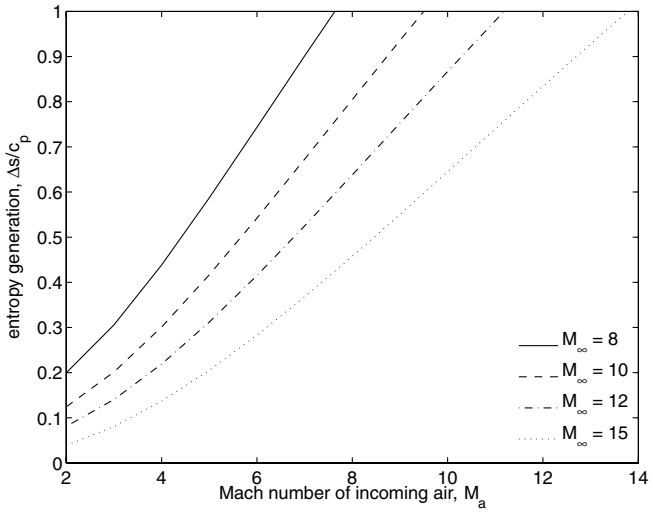

a) Variation in freestream condition

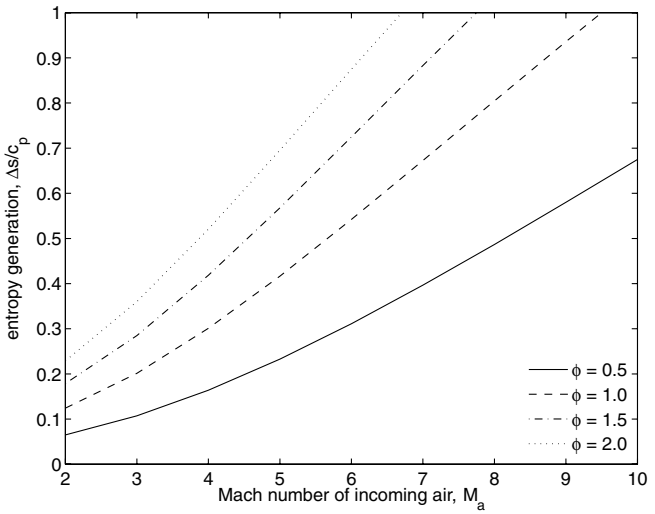

b) Variation in fuel equivalence ratio

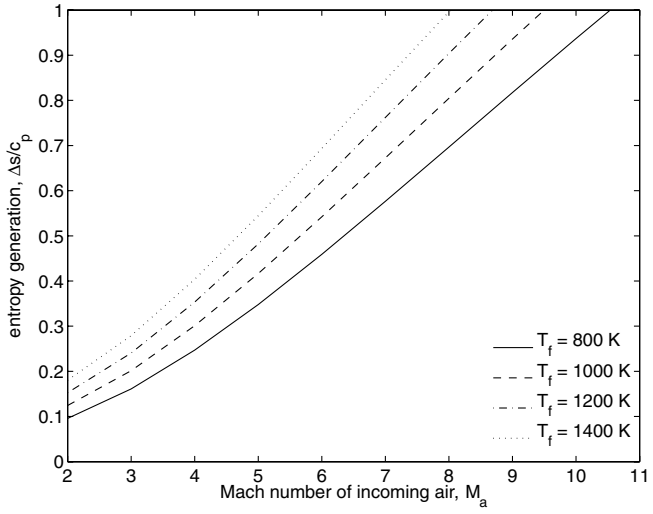

c) Variation in fuel injection temperature

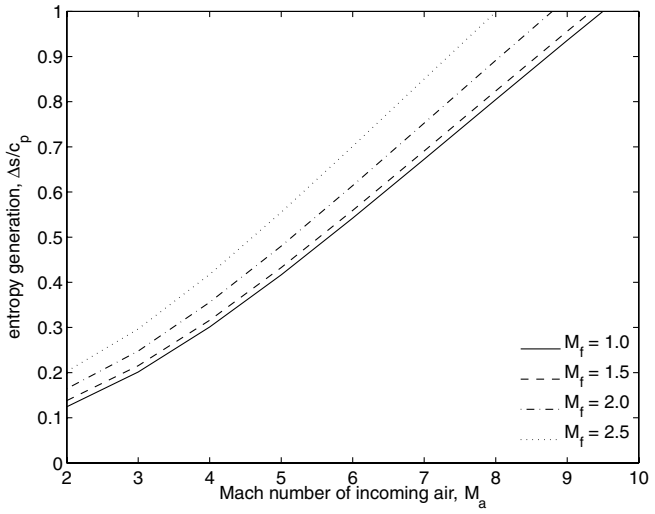

d) Variation in fuel injection Mach number

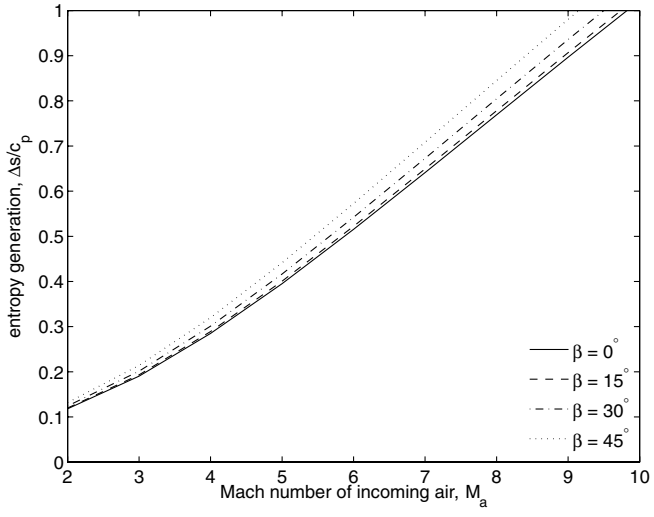

e) Variation in fuel injection angle

Fig. 7 Entropy generation from fuel injection for various properties.

of the external wedge angles) to find the configuration for the given flow conditions, and injection parameters gave the minimum entropy rise. The fuelling conditions at the injection location are as described previously.

The resulting thrust performance for the differing fuel arrangements where the fuel injection properties are taken from Table 3 can be seen in Fig. 10. The fuel equivalence ratios injected at locations along the inlet and in the combustor for the cases can be

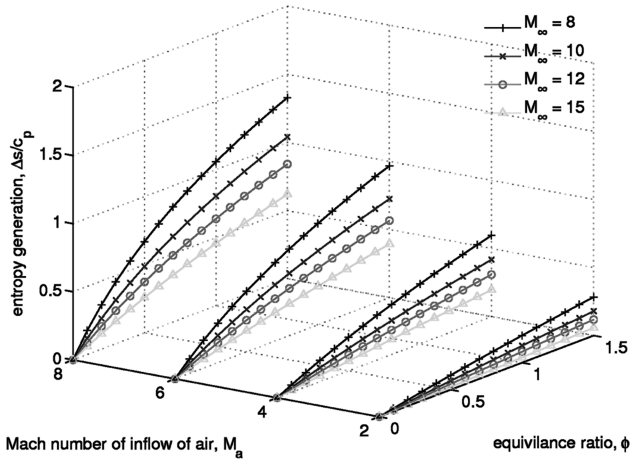

a) Variation in eqivalence ratio

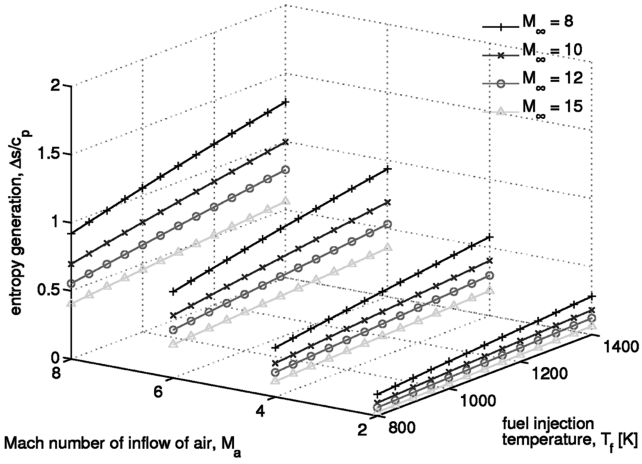

b) Variation in fuel temperature

Fig. 8 Entropy generation for differing freestream conditions with variation in inflow Mach number, M_a using nominal injection properties.

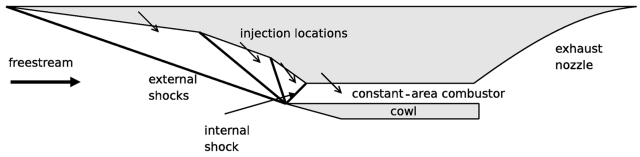

Fig. 9 Schematic of scramjet geometry with upstream injection.

seen in Table 4. This shows that the total entropy generated from fuel injection and mixing increases with the amount of fuel injected further upstream on the intake compared with the combustor. However, the entropy generated on the inlet is less with upstream injection due to the compression incurred by the fuel injection. Also, the pressure and temperature before combustion is found to exceed the 1000 K criteria. The combustion entropy generation is also slightly decreased due to the initially lower Mach number produced with the use of upstream injection.

Overall, there is not a huge difference in the total amount of entropy generated in the cycle, showing the intuitive result that combustor injection performs the best. However, with the thrust-per-unit intake area decreasing rapidly as entropy generation increases, there is a large effect of upstream injection on the overall thrust produced by the scramjet. A reduction of 40% if injected on the first wedge compared with that in the combustor. It can be seen that fuel injection upstream of the combustor may be best in limited amounts and closer to the combustor entrance where the local Mach number of the air has been reduced significantly from the freestream.

The thrust produced could be significantly lower if the frictional losses are included. For the conditions studied in Riggins et al. [11],

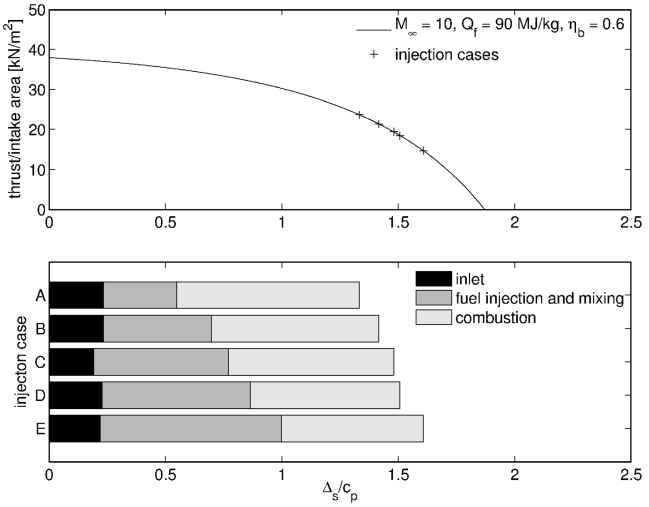

Fig. 10 Thrust performance for Mach 10 scramjet with differing fuel equivalence ratios at various injection locations along the inlet and combustor.

the total thrust in their Mach 12 scramjet example would be overestimated by 25% if not included. The overall effect, however, may be larger with upstream injection where the losses are higher before the combustion takes place. The amount of overall performance lost from upstream injection may be recovered from reduction in combustor skin friction if the combustor can be shortened.

V. Performance of Upstream Injection for Two-Dimensional Scramjet with Combustor Friction

To demonstrate the likely contribution to total entropy skin friction that the combustor will provide, analytical perfect gas calculations were performed on a constant-area duct with heat addition and friction [19]. The initial inflow conditions were set to be the same as those used previously (100 kPa static pressure, 1000 K static temperature, and a velocity of 2750 m/s) for the same Mach 10 freestream condition. The perimeter of the duct is 1 m, with a cross-sectional area of 0.04 m^2. The coefficient of skin friction is taken to be 0.005 and 0.01.

The modelling of heat release is implemented as a function of axial distance along the duct using Eq. (6). The combustion efficiency profile is shown in Fig. 11, where an initial period of no heat release occurs during mixing and ignition. It is assumed that the mixing length will be shorter and not affect the ignition length for the purpose of this study. Hydrogen and air are assumed to be perfectly mixed. Using the conditions at the start of the combustor, an ignition length of 0.591 m and reaction length of 0.26 m can be estimated using the correlations presented by Huber et al. [20]. With upstream injection, most of the mixing may occur upstream of the combustor, whereas in combustion injection an additional length is required before ignition may begin. Two cases are shown, with the length before reaction taken to be half of the predicted ignition length (0.295 m) and also the ignition length (0.591 m). During the reaction period, the heat is released as an exponential function of distance to 60% ($\eta_b = 0.6$) of the possible heat release.

$$q(x_c) = \lambda \eta_c(x_c) Q_f \tag{6}$$

Table 4 Fuel equivalence ratios injected at various locations for cases shown in Fig. 10

Case	First wedge	Second wedge	Third wedge	Combustor
A	0.0	0.0	0.0	1.0
B	0.0	0.0	0.5	0.5
C	0.0	0.0	1.0	0.0
D	0.0	1.0	0.0	0.0
E	1.0	0.0	0.0	0.0

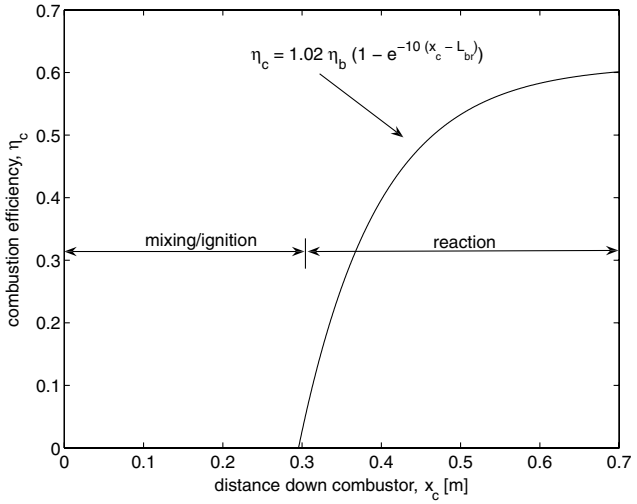

a) L_{br} = 0.295 m

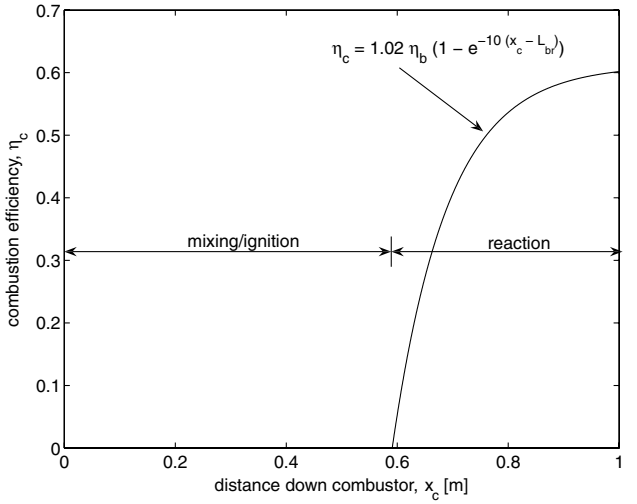

b) L_{br} = 0.591 m

Fig. 11 Combustion efficiency axially through combustor.

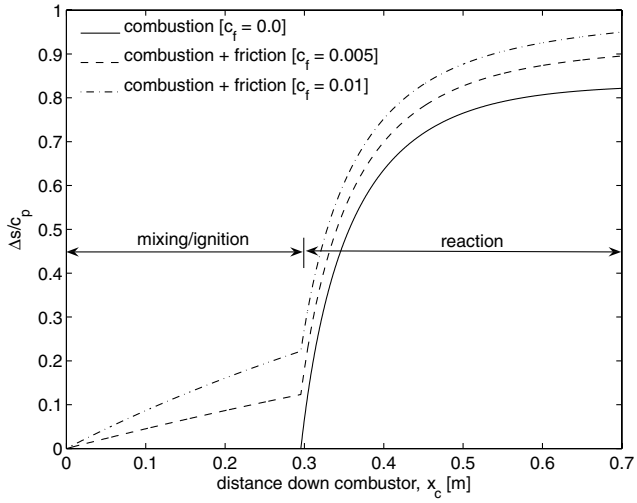

a) L_{br} = 0.295 m

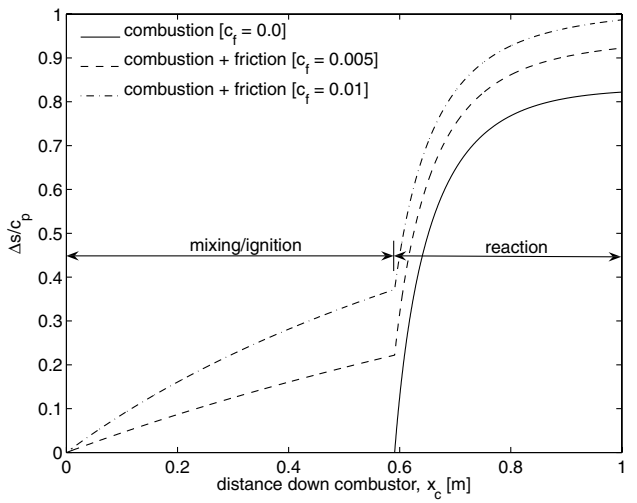

b) L_{br} = 0.591 m

Fig. 12 Entropy generation from supersonic combustion with friction along a constant-area duct.

With these heat addition profiles, the entropy rise through the combustor is shown in Fig. 12. Before any heat is added to the duct, the effect of the friction is seen to increase the entropy quite significantly. However, this reduces the entropy generated through the heat addition process compared with the inviscid case. There is only a slight increase in overall entropy generation with the length before reaction. This is demonstrated for a range of lengths before reaction in Fig. 13. Within the limitations of this simple analysis, upstream injection on the third wedge would need to reduce the length before reaction by approximately 1.5 times the ignition length (1.5 m) to achieve the same thrust as in the combustor injection case, if combustion is not mixing limited.

VI. Conclusion

The injection of fuel upstream of the combustor may be an attractive method for reducing combustor lengths due to increased mixing. However, the associated losses due to injection of the fuel into a higher Mach number must be assessed. Upstream injection losses have been shown to be quite significant in terms of overall performance and are quite dependent on fuel temperature, Mach number, and airstream total enthalpy. It has also highlighted the importance in ground testing for heated fuel systems, to ensure accuracy of thrust measurements. For an operational scramjet, optimization of the inlet to integrate the fuel injection can limit the overall flow losses, however, in this situation inviscid losses are still greater than if the fuel was injected into the combustor. This difference may be small enough to be recovered with shortening of the combustor, however, this will depend on the scramjet design and

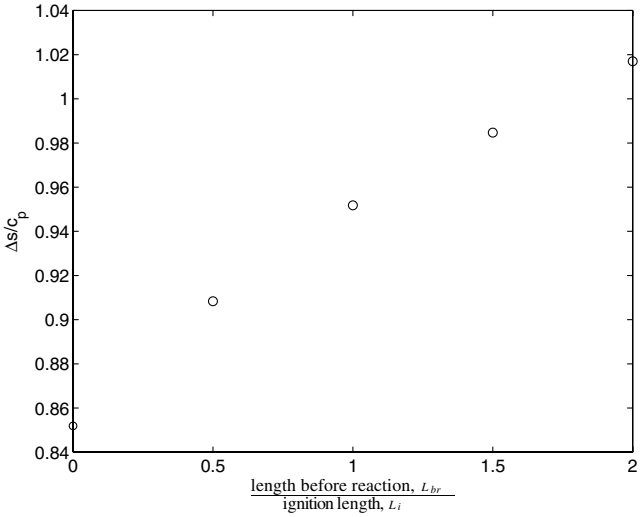

Fig. 13 Entropy generation from supersonic combustion with friction in a constant-area duct for various lengths before reaction ($c_f = 0.01$).

magnitude of mixing length reduction in the combustor. The analysis presented represents a useful technique for understanding the various counteracting phenomena involved in the location of the fuel injection station and for rapidly evaluating and optimizing candidate configurations before doing detailed numerical simulations.

Appendix A: Thrust Performance for Overall Scramjet Performance

The thrust-per-mass flow rate captured by a scramjet can be derived as shown in Eq. (3) if the pressure and area across the scramjet remains constant (i.e., $p_4 = p_1$ and $A_4 = A_1$). With replacing the velocity upon exit with $U_4 = M_4/\sqrt{\gamma RT_4}$, the Mach number upon exit can be calculated using Eq. (A2). This also requires the stagnation temperature upon exit, which can be calculated for the conservation, where the only addition is due to the mass addition and combustion of the fuel (i.e., $[(1 + \lambda\phi)H_4 = H_1 + \lambda\phi\eta_b Q_f]$). Rearrangement of this gives Eq. (A3). The temperature at exit can be given in terms of the entropy change across the engine ($\Delta s = \int_1^4 c_p \frac{\mathrm{d}T}{T} - R\,\ell_n(\frac{p_4}{p_1})$), where there is no change in pressure [Eq. (A4)]. Combining all of these gives Eq. (3) were the thrust is a function of the entropy generated through the flow processes within the scramjet

$$\frac{T}{\dot{m}_1} = (1 + \lambda\phi)U_4 - U_1 \tag{A1}$$

$$M_4 = \left[\left(\frac{T_{s,4}}{T_4} - 1\right)\frac{2}{\gamma - 1}\right]^{1/2} \tag{A2}$$

$$T_{s,4} = \frac{1}{1 + \lambda\phi}\left(T_{s,1} + \frac{\eta_b\lambda\phi Q_f}{c_p}\right) \tag{A3}$$

$$T_4 = T_1 e^{\frac{\Delta s}{c_p}} \tag{A4}$$

A correction must be made to the thrust as the exit area should not exceed the intake area due to external drag considerations. Firstly, a calculation must be made of the current exit area by using the conservation of mass [Eq. (A5)]. With this, the Mach number at the new exit M_4' can be calculated using the area ratios calculated for the Mach 1 conditions (i.e., $\frac{A_4}{A_1} = \frac{A_4}{A_*}\frac{A_*}{A_4}$). With the Mach number both the temperature and pressure can be found using the total temperature and total pressure at the original exit. It should be noted that the thrust now will be taken in reference to the intake area

$$\frac{A_4}{A_1} = \frac{\rho_1 U_1(1 + \lambda\phi)}{\rho_4 U_4} \tag{A5}$$

Appendix B: Entropy Generation for Injection and Mixing

Using the continuity, axial momentum, and energy equations [Eqs. (B1–B3)] the overall entropy change can be calculated across the injection and mixing region [as in Eq. (A4)] for a calorically perfect gas. With constant-pressure analysis, the entropy change is given simply by the temperature ratio over the region. Rearranging the energy equation and the continuity equation for the exit temperature ($H_b = c_{p,b}T_b + \frac{U_b^2}{2}$) gives Eq. (B4). This requires the velocity at the exit, which can be calculated by rearrangement of the axial momentum and continuity equation to give Eq. (B5). Therefore, the overall entropy change for constant-pressure mixing is given by Eq. (5)

$$\text{continuity}: \rho_a U_a A_a + \dot{m}_f = \rho_2 U_b A_b \tag{B1}$$

$$\text{axial momentum}: \rho_a U_a^2 A_a + \dot{m}_f U_f \cos\beta = \rho_b U_b^2 A_b \tag{B2}$$

$$\text{energy}: \rho_a U_a A_a H_a + \dot{m}_f H_f = \rho_b U_b A_b H_b \tag{B3}$$

$$T_b = \frac{1}{c_{p,b}}\left(\frac{H_a + \phi\lambda H_f}{1 + \phi\lambda} - \frac{U_b^2}{2}\right) \tag{B4}$$

$$U_b = \frac{U_a(1 + \phi\lambda U_f/U_a\cos\beta)}{1 + \phi\lambda} \tag{B5}$$

Acknowledgment

The authors would like to thank the Australian Research Council for providing the funding for Matthew McGilvray's Ph.D. scholarship.

References

[1] Sislian, J., *Scramjet Propulsion of Progress in Astronautics and Aeronautics: Detonation-Wave Ramjets*, AIAA, Reston, VA, Vol. 189, 2000, pp. 823–889, Chap. 13.

[2] Turner, J., and Smart, M., "Experimental Investigation of Inlet Injection in a Scramjet with Rectangular to Elliptical Shape Transition," *26th International Symposium on Shock Waves*, Göttingen, Germany, Paper 3642, 2007.

[3] Kumar, A., Bushnell, D., and Hussaini, M., "Mixing Augmentation Technique for Hypervelocity Scramjets," *Journal of Propulsion and Power*, Vol. 5, No. 5, Sept.–Oct. 1989, pp. 475–476.

[4] Van Wie, D., *Scramjet Propulsion of Progress in Astronautics and Aeronautics: Scramjet Inlets*, AIAA, Reston, VA, Vol. 189, 2000, pp. 447–511, Chap. 7.

[5] Morgan, R., Brescianini, C., Paull, A., Morris, N., and Stalker, R., "Shock Induced Ignition in a Model Scramjet," *Third National Space Engineering Symposium*, Institution of Engineers, Canberra, Australia, 1987, pp. 26–30.

[6] McGilvray, M., "Scramjet Testing at High Enthalpies in Expansion Tube Facilities," Ph.D. Thesis, University of Queensland, St. Lucia, Australia, 2008.

[7] Kovachevich, A., Paull, A., and McIntyre, T., "Investigation of an Intake Injected Hot-Wall Scramjets," AIAA Paper 2004-1037, Jan. 2004.

[8] Waltrup, P., Billig, F., and Stockbridge, R., "A Procedure for Optimizing the Design of Scramjet Engines," *Journal of Spacecraft and Rockets*, Vol. 16, No. 3, 1979, pp. 163–171.

[9] Ikawa, H., "Rapid Methodology for Design and Performance Prediction of Integrated Supersonic Combustion Ramjet," *Journal of Propulsion and Power*, Vol. 7, No. 3, May–June 1991, pp. 437–444.

[10] Kerrebrock, J., "Some Readily Quantifiable Aspects of Scramjet Performance," *Journal of Propulsion and Power*, Vol. 8, No. 5, Sept.–Oct. 1992, pp. 1116–1122.

[11] Riggins, D., McClinton, C., and Vitt, P., "Thrust Losses in Hypersonic Engines Part 1: Methodology," *Journal of Propulsion and Power*, Vol. 13, No. 2, March–April 1997, pp. 281–287.

[12] Riggins, D., "Thrust Losses in Hypersonic Engines Part 2: Applications," *Journal of Propulsion and Power*, Vol. 13, No. 2, March–April 1997, pp. 288–295.

[13] Curran, E., Leinang, J., Carreiro, L., and Petters, D., "Further Studies of Kinetic Energy Methods in High Speed Ramjet Cycle Analysis," AIAA Paper 92-3805, July 1992.

[14] Heiser, W., and Pratt, D., *Hypersonic Airbreathing Propulsion*, AIAA Education Series, AIAA, Washington, D.C., 1994.

[15] Builder, C., "On the Thermodynamic Spectrum of Airbreathing Propulsion," AIAA Paper 64-243, 1964.

[16] Kors, D., "Design Consideration for Combined Air Breathing-Rocket Propulsion Systems," *2nd International Aerospace Planes Conference*, AIAA Paper 90-5216, 1990.

[17] Ferri, A., "Review of SCRAMJET Propulsion Technology," *Journal of Aircraft*, Vol. 5, No. 1, 1968, pp. 3–10. doi:10.2514/3.43899

[18] Dunlap, R., Brehm, R., and Nicholls, J., "A Preliminary Study of the Application of Steady-State Detonation Combustion to a Reaction Scheme," *Journal of Jet Propulsion and Power*, Vol. 28, No. 6, 1958, pp. 451–456.

[19] John, J., *Gas Dynamics*, 2nd ed., Allyn and Bacon, Boston, 1983.

[20] Huber, P., Shenayder, C., Jr., and McClinton, C., "Criteria for Self-Ignition of Supersonic Hydrogen-Air Mixtures," NASA, Technical Paper 1457, 1979.

R. Bowersox
Associate Editor